Title	Possible method to observe the breathing mode of a magnetic domain wall in the Josephson junction
Author(s)	Michiyasu Mori, Wataru Koshibae, Shin-ichi Hikino and Sadamichi Maekawa
Citation	Journal of Physics; Condensed Matter, 26(25), 255702
Text Version	Author Accepted Manuscript
URL	https://jopss.jaea.go.jp/search/servlet/search?5046668
DOI	http://iopscience.iop.org/article/10.1088/0953-8984/26/25/255702/
Right	This is an Author's Accepted Manuscript of an article published in Journal of Physics; Condensed Matter 2014 © IOP Publishing Ltd, available online at: http://iopscience.iop.org/article/10.1088/0953-8984/26/25/255702/

Possible method to observe breathing mode of magnetic domain wall in Josephson junction

Michiyasu Mori

Advanced Science Research Center, Japan Atomic Energy Agency, Tokai, Ibaraki 319-1195, Japan

E-mail: `mori.michiyasu@jaea.go.jp`

Wataru Koshibae

RIKEN Center for Emergent Matter Science (CEMS), 2-1 Hirosawa, Wako, Saitama 351-0198, JAPAN

Shin-ichi Hikino

Computational Condensed Matter Physics Laboratory, RIKEN, Wako, Saitama 351-0198, Japan

Sadamichi Maekawa

Advanced Science Research Center, Japan Atomic Energy Agency, Tokai, Ibaraki 319-1195, Japan

Abstract. A magnetic domain wall (DW) behaves as a massive particle with elasticity. Sliding and oscillation of the DW have been observed experimentally, whereas vibration of a width in the DW, "*breathing mode*", has not been measured so far. We theoretically propose how to observe the breathing mode by the Josephson junction having a ferromagnetic layer between superconducting electrodes. The current-voltage (I-V) curve is calculated by an equivalent circuit of the resistively shunted junction model. The breathing mode is identified by stepwise structures in the I-V curve, which appear at the voltages $V = n(\hbar/2e)\omega$ with the fundamental constant $\hbar/e$, integer number n, and the frequency of the breathing mode ω.

PACS numbers: 74.50.+r,75.70.Kw,75.75.-c,85.25.Cp

Submitted to: *J. Phys.: Condens. Matter*

1. Introduction

A magnetic domain wall (DW) is a solitonic object which connects two stable configurations of magnetizations. Many studies are devoted to control the DW due to many advantages from an application viewpoint such as enhanced operation speed, low power consumption, and high density integration of electronic devices [1, 2, 3, 4, 5, 6, 7, 8, 9, 10, 11, 12, 13, 14]. Experimentally, it is shown that the DW behaves as a particle with finite mass [3, 4] and is driven by an electric current [5, 6]. Oscillation of the DW confined in a potential is studied experimentally [4, 7, 8, 9, 10] and theoretically [11, 12, 13, 14, 15]. In addition to the oscillation, a vibration of a width of the DW called "*breathing mode*" is expected, since this solitonic object is composed of many electron spins. In the previous theoretical studies [16, 17, 18, 19], the breathing mode induced by the electric current has been discussed. A current-driven breathing mode is expected to be a microwave source of wireless telecommunication devices [18, 19]. Experimentally, however, the method to detect and measure the breathing mode of DW has not been established so far.

Superconductors (SCs) provide many types of devices sensitive to an external magnetic field and are used for precise measurement of voltage [20, 21]. Superconducting quantum interference devices (SQUIDs) presently offer the highest sensitivity to a magnetic field. The Josephson junction under irradiation of microwave provides a precise value of voltage adopted to the voltage standard [22, 23]. In the latter case, the current-voltage (I-V) curve shows step structures at the voltage $V = n(\hbar/2e)f$ with microwave frequency f, integer n, and the ratio of the Planck constant and the elementary charge $\hbar/e$. This structure called Shapiro step [24] determines the voltage in the order of 10^{-9} accuracy, since the frequency of microwave and the fundamental constants are measured precisely [22, 23].

The Josephson junction composed of SCs and ferromagnet (FM) has been studied by many authors (see Refs.[25, 26] as review). In a *ferromagnetic Josephson junction* (FJJ), two superconducting electrodes are separated by a thin ferromagnetic layer. By irradiation of microwave, the I-V curve of the FJJ shows resonances similar to the Shapiro step [27, 28, 29, 30, 31, 32, 33]. It is noted that the resonances appear at the voltages $V = n(\hbar/2e)\Omega$ with ferromagnetic resonance frequency Ω [27]. Hence, we can see the magnetic response in the ferromagnet by the I-V curve of the FJJ [34, 35].

In this paper, we theoretically propose the method to observe the breathing mode of the DW by the FJJ, which has a ferromagnetic layer with the DW between two SCs. An equivalent circuit of resistively shunted junction (RSJ) model is used to calculate the I-V curve. In §2, equations of motion for the DW and breathing mode of DW are introduced. In §3, the equivalent circuit of RSJ model is derived by considering the DW in the FJJ, and the I-V curve is numerically calculated. In addition to the breathing mode, the oscillation of the DW is also examined. In §4, results are summarized.

2. Oscillation and Breathing Mode of Magnetic Domain Wall

To determine the magnetic domain structure, the geometrical anisotropy is of crucial importance. In this paper, we suppose permalloy for the FM and the junction system with the condition $L_x > L_z$. In such a nano-wire structure of permalloy, the head-to-head magnetic-domain-structure, which is schematically shown in Fig. 1, is stabilized ‡. By external stimuli, the DW shows a dynamics. In the one-dimensional model,

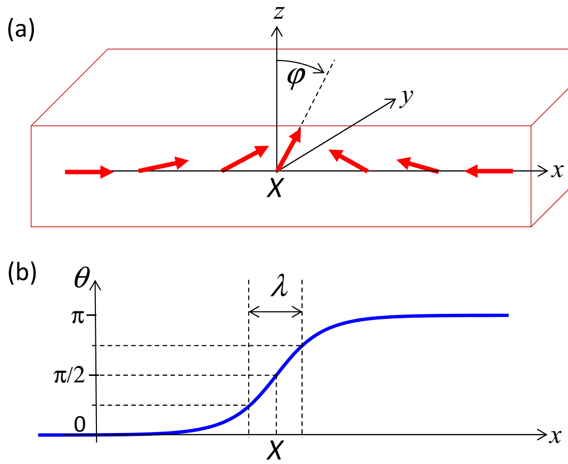

Figure 1. (Color online) (a) Schematic figure of DW in the FM (rectangle). The red arrows indicate the spatial dependence of the magnetization. A position of the DW is denoted by X, and φ is the tilting angle of the magnetic moment at X from the easy plane (x-z plane) to the hard axis (y axis). (b) Spatial dependence of magnetization determined by an angle $\theta = \cos^{-1}[\tanh\{(x - X)/\lambda\}]$, which is the angle between the magnetic moment and x axis.

the equation of motion of the DW trapped in pinning potential $V \equiv \beta X^2$ is given by [1, 2, 13, 14, 16, 17, 18, 19],

$$\frac{d\varphi}{dt} + \frac{\alpha}{\lambda}\frac{dX}{dt} = -\beta X, \tag{1}$$

$$\frac{dX}{dt} - \alpha\lambda\frac{d\varphi}{dt} = \frac{S}{2\hbar}\lambda K_\perp \sin 2\varphi, \tag{2}$$

$$\alpha\frac{\pi^2}{12}\frac{d\lambda}{dt} = \frac{S}{2\hbar}\left\{\frac{J}{\lambda} - \left(K + K_\perp \sin^2\varphi\right)\lambda\right\}, \tag{3}$$

where X is the position of the DW with magnitude of spin S. The structure of DW is determined by magnetic exchange energy J, easy-axis anisotropy K and hard-axis one $K_\perp$. Then, the one-dimensional DW with width λ is given by $\theta = \cos^{-1}[\tanh\{(x - X)/\lambda\}]$ as a function of spatial coordinate x. To obtain the breathing mode, the Gilbert damping constant α is necessary. Here, we note the following two

‡ As discussed in the next section, the magnetic flux is restricted in the junction area due to the superconducting diamagnetic current. The hard axis is also brought about by such a junction geometry.

limiting cases [13]; weak pinning case, $V \ll K_\perp$ and strong pinning case, $V \gg K_\perp$. In the former case, $\varphi \sim 0$ and we obtain the equation of motion for X given by,

$$(1+\alpha^2)\frac{d^2X}{dt^2} + \alpha\left(\lambda\beta + \frac{S}{\hbar}K_\perp\right)\frac{dX}{dt} + \lambda\beta\frac{S}{\hbar}K_\perp X = 0, \tag{4}$$

where the DW is associated with an oscillating particle in the pinning potential [3, 4]. This case is relevant to our previous study [15]. On the other hand, in the latter case, the DW is strongly confined around the potential-center (i.e., $X \sim 0$) and the equation of motion for φ is obtained as,

$$(1+\alpha^2)\frac{d^2\varphi}{dt^2} + \alpha\left(\lambda\beta + \frac{S}{\hbar}K_\perp \cos 2\varphi\right)\frac{d\varphi}{dt} + \lambda\beta\frac{S}{2\hbar}K_\perp \sin 2\varphi = 0. \tag{5}$$

This results in a rotation or oscillation with respect to the easy-axis. Note that the oscillation of φ induces the breathing mode due to Eq. (3) (See Refs. [16, 17, 18, 19]). This naturally derived breathing of the DW has not been much discussed experimentally, because of difficulty to build observation technique. In the next section, we propose a method sensitive to the breathing mode of the DW.

3. Equivalent Circuit of RSJ Model with Magnetic Domain Wall

For a conventional Josephson junction, where two SCs are separated by a thin insulating barrier, an equivalent circuit of Josephson junction with the bias current I (RSJ model) is given by,

$$I = \frac{V}{R} + I_{\mathrm{J}} = \frac{1}{R}\frac{\Phi_0}{2\pi}\frac{d\phi}{dt} + J_{\mathrm{c}}\sin\phi. \tag{6}$$

Here, the Josephson relation $d\phi/dt = (2e/\hbar)V$ and the flux quantum $\Phi_0 \equiv h/2e$ are used. In the RSJ model, the Josephson junction is associated with a parallel circuit composed of a resistance R and a Josephson current $I_{\mathrm{J}} \equiv J_{\mathrm{c}}\sin\phi$ with the Josephson critical current J_{c}. Because of the gauge invariance in a magnetic field, the phase difference ϕ gets the additional term $2\pi\Phi/\Phi_0$ as $\phi \to \phi + 2\pi\Phi/\Phi_0$, where Φ is the magnetic flux through the junction (See Refs.[20, 21]).

We consider the FJJ with DW as shown in Fig. 2 (a) §. The interface is parallel to the xz-plane with width L_x and height L_z. A dc bias current is applied in the y-direction between the superconducting electrodes separated by depth L_y. The magnetic flux densities B due to the DW is supposed as shown in Figs. 2 (b) and (c), where M_{S} is the saturation magnetization and x_1 and x_2 are both ends of the DW. Considering the magnetic flux densities induced by the DW through the junction, I_{J} is given by,

$$\begin{aligned}\frac{I_{\mathrm{J}}}{J_c} = &\left(\frac{1}{2}+x_1\right)\frac{\sin(\pi\phi_x)}{\pi\phi_x}\sin\left(\phi - \pi\phi_z\lambda\right)\\ &+ \frac{\sin\left(\pi\phi_z\lambda\right)}{\pi\phi_z}\sin\left(\phi\right)\end{aligned}$$

§ This simplified structure of DW captures its essential properties and does not change our conclusion.

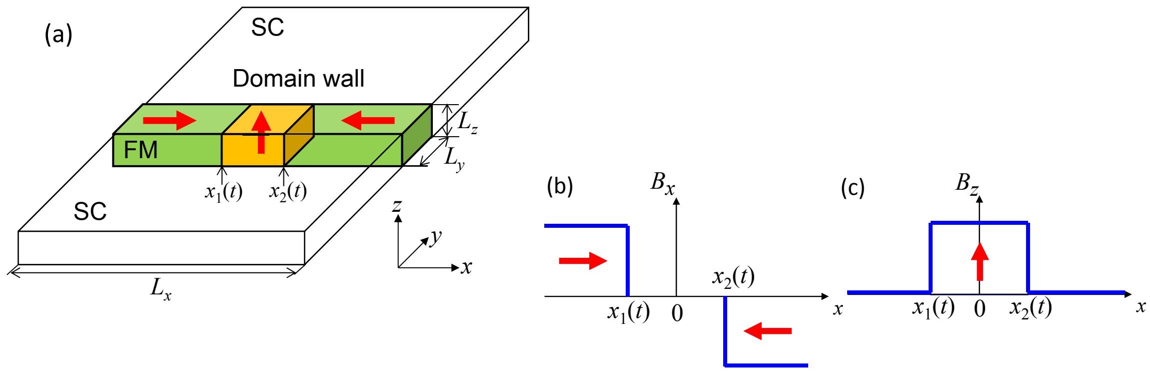

Figure 2. (Color online) (a) Schematic of an oscillating domain wall in a ferromagnetic layer (FM) that separates two superconductors (SCs). Magnetic structure of the FM is shown by the red arrows. A dc bias current I in the y-direction induces a time-dependence of the Josephson phase ϕ. An ac bias current, which induces a breathing mode and/or oscillation of DW is applied to the x-direction. (b) The x-component and (c) the z-component of magnetic fields.

$$+ \left(\frac{1}{2} - x_2\right) \frac{\sin(\pi\phi_x)}{\pi\phi_x} \sin(\phi + \pi\phi_z\lambda) \tag{7}$$

$$= \left[(1-\lambda)\frac{\sin(\pi\phi_x)}{\pi\phi_x}\cos(\pi\phi_z\lambda) + \frac{\sin(\pi\phi_z\lambda)}{\pi\phi_z}\right]\sin(\phi)$$
$$- 2x_0\frac{\sin(\pi\phi_x)}{\pi\phi_x}\sin(\pi\phi_z\lambda)\cos(\phi)\,, \tag{8}$$

with $\phi_i \equiv \Phi_i/\Phi_0$ $(i = x,\, z)$, and $\Phi_x \equiv L_y L_z M_{\mathrm{S}}$, $\Phi_z \equiv L_x L_y M_{\mathrm{S}}$ [15]. The position of the DW is scaled by L_x and $x_1, x_2 \in [-1/2, 1/2]$ in units of L_x. In Eq. (7), the first and third terms originate from B_x in the regions $x \le x_1$ and $x_2 \le x$, respectively, while the second term is obtained by B_z [15, 20, 21]. In Eq. (8), $(x_1+x_2)/2 \equiv x_0$ and $x_2 - x_1 \equiv \lambda$ are used. Note that Eq. (8) contains the term proportional to the cosine function, whereas the critical current in the conventional Josephson junction is proportional to the sinusoidal function with respect to the phase difference. The interference of two contributions by the left and the right regions on both sides of the DW is the origin of this term and hence its magnitude is determined by the position of the DW, x_0. Below, it is assumed that the width of the DW λ is smaller than L_x. In the case without DW, i.e., $\lambda = 0$, the Josephson critical current depends on the magnetic field in a similar way to the Fraunhofer diffraction pattern as, $J_c \sin(\pi\phi_x)/(\pi\phi_x)$. In another case with $\lambda = 1$, $J_c \sin(\pi\phi_z)/(\pi\phi_z)$ is obtained. In both limits, Eq. (8) reproduces the Fraunhofer diffraction pattern about the magnetic-field dependence on the Josephson critical current.

We numerically solve the RSJ model with Eq. (8) and calculate the I-V curve by $V = (\hbar/2e)\langle d\phi/dt\rangle$ [20, 21]. The bracket means the time average, i.e., $\langle d\phi/dt\rangle = (1/T)\int_0^T dt(d\phi/dt)$. We examine the following three cases: (i) The position of DW is oscillating with a frequency ν, i.e. $X = x_0 + \delta x_0 \sin(\nu t)$ and $\lambda = \lambda_0$ [15], namely we assume the oscillation around x_0 with an amplitude δx_0. This emulates the weak pinning case, (see the discussions with Eq. (4)). (ii) The width of DW is vibrating with a frequency ω, i.e., $X = x_0$ and $\lambda = \lambda_0 + \delta\lambda \sin(\omega t)$, where λ_0 is the mean width of the DW and $\delta\lambda$ ($< \lambda_0/2$) is the amplitude of the vibration. This is the breathing mode and is related to the strong pinning case (see the discussions with Eq. (5)). (iii) Both of X and λ are time-dependent, i.e., $X = x_0 + \delta x_0 \sin(\nu t)$ and $\lambda = \lambda_0 + \delta\lambda \sin(\omega t)$‖.

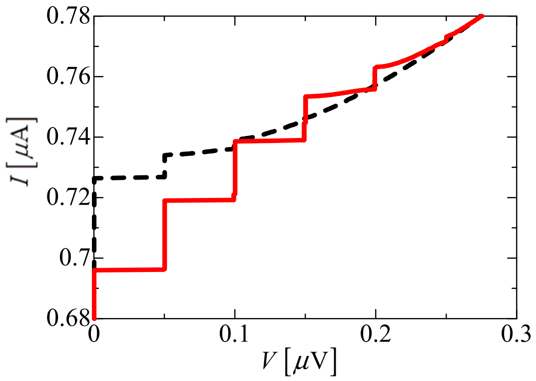

Figure 3. (Color online) The I-V curves of the cases (i) $X = x_0 + \delta x_0 \sin(\nu t)$, $\lambda = \lambda_0$ and the case (ii) $X = x_0$, $\lambda = \lambda_0 + \delta\lambda \sin(\omega t)$ are shown by the broken (black) and solid lines (red), respectively, for $x_0 = 0.05$, $\delta x_0 = 0.1$, $\lambda_0 = 0.2$, $\delta\lambda = 0.05$, and $\nu\tau_0 = \omega\tau_0 = 0.05$. Steps appear at $V = m(\hbar/2e)\nu$ and $V = n(\hbar/2e)\omega$ and with integer m and n. Note the relation $V/(J_c R) = n(\omega\tau_0)$ with $(\hbar/2e)(1/J_c R) \equiv \tau_0$.

In Fig. 3, the I-V curves of the cases (i) and (ii) are shown by the broken (black) and solid (red) lines, respectively, for $\nu\tau_0 = \omega\tau_0 = 0.05$ with $\tau_0 \equiv (\hbar/2e)(1/J_c R)$. This corresponds to a frequency $\omega = \nu = 152$ MHz for the parameters, L_x=500 nm, L_y=5 nm, L_z=200 nm, J_c=1 μA, R=1 Ω, M_S=0.75 T, $x_0 = 0.05$, $\delta x_0 = 0.1$, $\lambda_0 = 0.2$, and $\delta\lambda = 0.05$. We find the step structures at $V = m(\hbar/2e)\nu$ in the broken line (black) and $V = n(\hbar/2e)\omega$ in the solid line (red). Note that the step in the solid line (red) is much more clear than that in the broken line (black), even though the magnitude of $\delta x_0 = 0.1$ is twice as that of $\delta\lambda = 0.05$. Therefore, our method is quite sensitive to the breathing mode of the DW. Furthermore, our result relates V to ω (ν) with the fundamental constant $\hbar/e$ [38] ¶ and integer n. On the other hand, V is precisely determined by the conventional Josephson junction in the order of 10^{-9} accuracy [22, 23]. The measurement on V determines ω precisely. In addition, the Josephson junction has the highest sensitivity to a magnetic field in the order of femtotesla and the highest speed of switching in the order of tens picosecond [20, 21]. Therefore, our method is a powerful method to observe the breathing mode of the DW.

‖ References [16, 17, 18, 19] show the monochromatic oscillation of the DW by applying the electric current. The oscillation will survive even if the Josephson current flows perpendicular to the applied current, since the magnitude of Josephson current is two or three orders of magnitude smaller than the applied one [4].

¶ Accuracy is in the order of 10^{-10}, e.g., e=1.602 176 487(40) $\times$ 10^{-19}C and $\hbar$=1.054 571 628(53) $\times$ 10^{-34}J·s.

Figure 4 shows a result of I-V curve for the case (iii) with $\nu\tau_0 = 0.05$ and $\omega\tau_0 = 0.08^+$. Again, we find the step structures at $V = n(\hbar/2e)\omega$ (due to the breathing

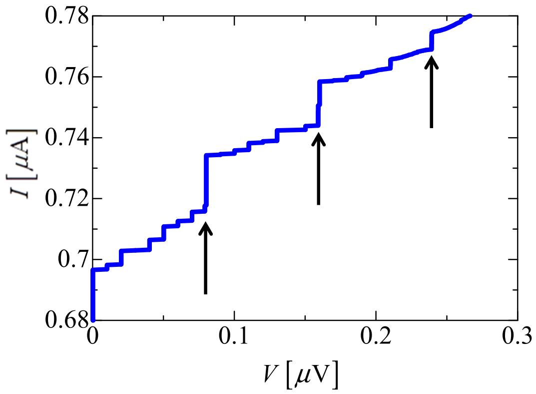

Figure 4. (Color online) The I-V curves of the case (iii) $X = x_0 + \delta x_0 \sin(\nu t)$ and $\lambda = \lambda_0 + \delta\lambda \sin(\omega t)$, for $x_0 = 0.05$, $\delta x_0 = 0.1$, $\lambda_0 = 0.2$, $\delta\lambda = 0.05$, $\nu\tau_0 = 0.05$ and $\omega\tau_0 = 0.08$. The steps occur at $V = (n\omega + m\nu)(\hbar/2e)$ with integers n and m, and the breathing mode is clearly found at the large steps noted by the arrows, which correspond to $V = n\omega(\hbar/2e)$ with n=1, 2, and 3.

of the DW) and $m(\hbar/2e)\nu$ (due to the oscillation of the position of the DW). However, the number of steps is more than expected. For example, the step appears at V= 0.02, 0.06, and so on. These correspond to $V = (\hbar/2e)(n\omega + m\nu)$ with integers m and n: Here, we consider the following term to elucidate the steps in the I-V curve,

$$\sin(\nu t)\sin(\omega t)\cos(\phi), \tag{9}$$

which is involved in Eq. (8). Because of this time-dependent term, the solution of Eq. (6) with Eq.(8) contains the component given by,

$$\phi = (\frac{2e}{\hbar})Vt + A\sin(\omega t) + B\sin(\nu t), \tag{10}$$

where A and B are constants. Considering Eq. (10), we find that Eq. (9) is composed of the following terms,

$$e^{\pm i\phi \pm i(\omega\pm\nu)t} = \sum_{n,m=-\infty}^{\infty} J_n(A)\, J_m(B)\, e^{i(2e/\hbar)Vt - in\omega t - im\nu t}, \tag{11}$$

where $J_n(A)$ and $J_m(B)$ are the Bessel functions of the first kind. The step structures are associated with the dc component of I_J, which is given by taking the time average of Eq. (8). Then, the constant term in Eq. (11), i.e., time-independent term, gives the step structure in the I-V curve. Therefore, we find the condition $(2e/\hbar)V - n\omega - m\nu = 0$ for the step structures. In particular, the steps appear at V= 0.02, and 0.06 for (n, m)=$(-1, 2)$, and $(2, -1)$, respectively. Although the step structures due to the oscillation and the breathing mode of the DW are mixed up in the I-Vcurve, the

+ Here, we examine more general case with $\nu \neq \omega$, although Eqs (1), (2) and (3) based on the one-dimensional model result in $\nu = \omega$.

breathing mode can be identified by the large steps even in the case (iii) as noted by the arrows in Fig. 4.

4. Summary and Discussions

We have theoretically proposed how to observe the breathing mode of DW by the Josephson junction having a ferromagnetic layer with the magnetic domain wall between superconducting electrodes. The current-voltage (I-V) curve is calculated by an equivalent circuit of the resistively shunted junction model. The breathing mode is identified by stepwise structures in the I-V curve, which appear at the voltages $V = n(\hbar/2e)\omega$ with the fundamental constant $\hbar/e$, integer number n, and the frequency of the breathing mode ω. This is the most feasible method to observe the breathing mode of the DW due to the sensitivity of the Josephson junction.

In principle, magnetic resonance methods are also possible to measure the breathing mode. Owing to their low sensitivity, however, the resonance measurements need a sample containing a number of DWs, and furthermore those DWs need to vibrate collectively. Although such a measurement is realized in the Skyrmion lattice [39, 40], in which the rotational and the breathing modes are observed, it has not been done on the breathing mode of the DW so far. On the other hand, our method is accessible to the breathing mode of a single DW due to the sensitivity of the Josephson junction [20, 21].

Acknowledgments

The authors would like to thank J. Ieda for useful discussions and comments. This work was partly supported by Grant-in-Aid for Scientific Research from MEXT (Grant No.24540387, No.24360036, No.23340093, and No.25287094) and by the inter-university cooperative research program of IMR, Tohoku University. Numerical computation in this work was carried out on the supercomputers at JAEA.

References

[1] S. Chikazumi, *Physics of Ferromagnetism* (Oxford University Press, New York, 1997).
[2] S. Maekawa, *Concepts in Spin Electronics* (Oxford University Press, Oxford, 2006).
[3] W. Döring, Z. Naturforsch **3A** 373 (1948).
[4] E. Saitoh, H. Miyajima, T. Yamaoka, G. Tatara, Nature **432**, 203 (2004).
[5] M. Yamanouchi, D. Chiba, F. Matsukura, and H. Ohno, Nature **428**, 539 (2004).
[6] A. Yamaguchi, T. Ono, S. Nasu, K. Miyake, K. Mibu, and T. Shinjo, Phys. Rev. Lett. **92**, 077205 (2004).
[7] L. Thomas, M. Hayashi, X. Jiang, R. Moriya, C. Rettner and S. Parkin, Nature **443**, 197 (2006).
[8] M. Hayashi, L. Thomas, C. Rettner, R. Moriya and S. S. P. Parkin, Nature Physics **3**, 21 (2007).
[9] C. T. Boone, J. A. Katine, M. Carey, J. R. Childress, X. Cheng, and I. N. Krivorotov, Phys. Rev. Lett. **104**, 097203 (2010).
[10] A. Bisig, L. Heyne, O. Boulle, M. Kläui, Appl. Phys. Lett. **95**, 162504 (2009).
[11] A. Thiaville, J. M. García, and J. Miltat, J. Magn. Magn. Mater. **242-245**, 1061 (2002).
[12] J. He and S. Zhang, Appl. Phys. Lett. **90**, 142508 (2007).

[13] G. Tatara, H. Kohno, and J. Shibara, Phys. Rep. **468**, 213 (2008).
[14] J. Ieda, H. Sugishita, and S. Maekawa, J. Magn. Magn. Mat. **322**, 1363 (2010).
[15] S. Hikino, M. Mori, W. Koshibae, and S. Maekawa, Appl. Phys. Lett. **100**, 152402 (2012).
[16] A. L. Dantas, M. S. Vasconcelos, and A.S. Carriço, J. Magn. Magn. Mater. **226-230**, 1604 (2001).
[17] S. W. Jung and H. W. Lee, J. Magnetics **12**, 1 (2007).
[18] K. Matsushita, J. Sato, and H. Imamura, J. Phys. Soc. Jpn. **78**, 093801 (2009).
[19] K. Matsushita, M. Sasaki, J. Sato, and H. Imamura, J. Phys. Soc. Jpn. **81**, 043801 (2012).
[20] A. Barone and G. Paternó, *Physics and Applications of the Josephson Effect* (Wiley, New York, 1982).
[21] M. Tinkham, *Introduction to superconductivity (Second Edition)* (Dover, New York, 2004).
[22] C. A. Hamilton, Rev. Sci. Instrum. **71**, 3611 (2000).
[23] J. Kohlmann, R. Behr, and T. Funck, Meas. Sci. Technol. **14**, 1216 (2003).
[24] S. Shapiro, Phys. Rev. Lett. **11**, 80 (1963).
[25] A. I. Buzdin, Rev. Mod. Phys. **77**, 935 (2005).
[26] F. S. Bergeret, A. F. Volkov, and K. B. Efetov, Rev. Mod. Phys. **77**, 1321 (2005).
[27] S. Hikino, M. Mori, S. Takahashi, and S. Maekawa, J. Phys. Soc. Jpn. **77** 053707 (2008).
[28] M. Houzet, Phys. Rev. Lett. **101**, 057009 (2008).
[29] F. Konschelle and A. Buzdin, Phys. Rev. Lett. **102**, 017001 (2009).
[30] I. Petković, M. Aprili, S. E. Barnes, F. Beuneu, and S. Maekawa, Phys. Rev. B **80**, 220502 (2009).
[31] A. F. Volkov and K. B. Efetov, Phys. Rev. Lett. **103**, 037003 (2009).
[32] S. Hikino, M. Mori, S. Takahashi, and S. Maekawa, Physica C **470**, S819 (2010).
[33] S. Hikino, M. Mori, S. Takahashi, and S. Maekawa, Supercond. Sci. Technol. **24**, 024008 (2011).
[34] S. Hikino, M. Mori, S. Takahashi, and S. Maekawa, J. Phys. Soc. Jpn. **80**, 074707 (2011).
[35] S. Hikino, M. Mori, and S. Maekawa, arXive:1306.3652
[36] J. J. Versluijs, M. A. Bari, and J. M. D. Coey, Phys. Rev. Lett. **87**, 026601 (2001).
[37] S. E. Barnes, J. Ieda, and S. Maekawa, Appl. Phys. Lett. **89**, 122507 (2006).
[38] P. J. Mohr, B. N. Taylor, and D. B. Newell, Rev. Mod. Phys. **80**, 633 (2008).
[39] Y. Onose, Y. Okamura, S. Seki, S. Ishiwata, and Y. Tokura, Phys. Rev. Lett. **109**, 037603 (2012).
[40] M. Mochizuki, Phys. Rev. Lett. **108**, 017601 (2012).